Critical dimension of the transition from single switching to an exchange spring process in hard/soft exchange-coupled bilayers

Shi-shen Yan,[1,*] J. A. Barnard,[2] Feng-ting Xu,[1] J. L. Weston,[1] and G. Zangari[1]
[1]*Center for Materials for Information Technology, The University of Alabama, Tuscaloosa, Alabama 35487-0209*
[2]*Department of Materials Science and Engineering, University of Pittsburgh, Pittsburgh, Pennsylvania 15261*
(Received 21 May 2001; published 12 October 2001)

Hard/soft exchange-coupled $Ni_{80}Fe_{20}/Sm_{40}Fe_{60}$ bilayers with well-defined induced in-plane uniaxial anisotropy were deposited on (100) Si and glass substrates by dc magnetron sputtering. The magnetization-reversal process was systematically studied by analyzing the magnetic hysteresis loops measured by the alternating-gradient magnetometer and surface-sensitive magneto-optic Kerr effect. The coercivity in the single-switching process and the nucleation field in the exchange spring process are quantitatively described by theoretical models. As a result, a critical dimension equation describing the transition from a single-switching process to an exchange spring process is developed. Different magnetization-reversal processes are essentially determined by the exchange length (or domain wall width) of the soft layer under an external field and the pinning energy exerted on the domain wall of the hard layer near the interface.

DOI: 10.1103/PhysRevB.64.184403 PACS number(s): 75.70.−i

I. INTRODUCTION

Exchange-coupled multilayers with alternating hard and soft magnetic layers are of great technological and scientific interest. They can be used as permanent magnets with giant magnetic energy production[1,2] or as giant magnetostrictive materials with low saturation field.[3,4] It is expected that during the magnetization-reversal process the magnetic moments in a thick soft magnetic layer rotate reversibly with the directions distributed successively depending on the distance from the hard/soft interface. This is the so-called exchange-spring phenomenon. Exchange spring multilayers serve as an ideal model system for studying the whole process of the nucleation, compression, decompression, and propagation of an artificial in-plane domain wall.[5–7] On the other hand, if both the soft layer and hard layer are thin, the magnetic moments in both layers are expected to couple together and reverse together under an external field,[8] due to the strong direct exchange interaction at the hard/soft magnetic layer interface.

The exchange spring phenomenon has been studied by many researchers.[2,5–7] It was found experimentally that the easy-axis nucleation field of the soft magnetic layer versus the thickness of the soft layer can be well described by the theoretical expression.[9,10]

$$H_N = H_{N0}/(t_s)^n, \tag{1}$$

where t_s is the thickness of the soft layer, and H_{N0} and n are two constants for the given hard/soft exchange-coupled system. If the soft layer has no anisotropy and the hard layer is perfectly rigid, theory[9] predicts $H_{N0}=\pi^2 A/2M_s$, and $n=2$, where A and M_s are, respectively, the exchange constant and the saturation magnetization of the soft layer. Further experimental and theoretical work[10] indicate $n=1.75$ for a thick soft layer without anisotropy and a hard layer with a definite anisotropy. The value of n $(n=1.75)$ is almost independent of the quantitative values of materials parameters.

Another characteristic field of the exchange spring phenomenon is the easy-axis irreversible switching field of the hard layer. Although the simple one-dimensional atomic model or the continuum approximation of micromagnetics can well describe the reversible magnetization reversal of the soft layer, they cannot predict correctly the irreversible switching field of the hard layer.[2,5–7,11] This is because these models only consider the rotation of the magnetization or the nucleation of the reversed domain. The magnetization reversal at the irreversible switching field of the hard layer is less well understood.

Although the behavior appears simple when the magnetizations of the thin soft layer and thin hard layer couple together and reverse together, the magnetization-reversal mechanisms still require further study. Recently we proposed a magnetization-reversal model[8] to describe the whole magnetization-reversal process by combining coherent rotation and domain-wall unpinning. When the external field is along the easy axis, the magnetization reversal is caused by domain-wall unpinning. When the external field is along or near the hard axis, the magnetization reversal is caused by coherent rotation. For other orientations, the magnetization first rotates gradually by coherent rotation and then sharply switches by domain-wall unpinning. The easy-axis coercivity versus the thicknesses of the soft layer and hard layer for soft/hard/soft trilayers[8] can be well described by an extended model of the conventional domain-wall unpinning, i.e.,

$$H_C = H_0 t_h/(t_h + 2\alpha t_s), \tag{2}$$

where H_0 can be regarded as the coercivity of the single hard layer of thickness t_h (the coercivity of the soft layer is negligible compared with H_0), $2t_s$ is the total thickness of the two soft layers, and $\alpha = M_s/M_h$ is the ratio of the magnetization of the soft layer to that of the hard layer. In the following we call this case the single switching field process to distinguish it from the exchange spring process characterized by two switching fields (the easy-axis nucleation field of the soft magnetic layer and the easy-axis irreversible switching field of the hard layer).

In spite of the many significant investigations of hard/soft exchange-coupled systems, no quantitative information is

known on the critical dimension of the transition from the single-switching-field process to the exchange spring process. In this article we attempt to clarify this situation by systematically studying the single-switching-field process and the exchange spring process.

II. EXPERIMENTS

$Ni_{80}Fe_{20}/Sm_{40}Fe_{60}$ bilayers of various thicknesses were prepared on (100) Si and glass substrates by dc magnetron sputtering at room temperature. The pressure of Ar gas was stabilized at 3 mTorr during the sputtering process. Unless specified, the results are obtained from samples deposited on (100) Si substrates. The deposition rates for NiFe and SmFe layers are 0.15 nm/s and 0.16 nm/ms, respectively. To induce an in-plane uniaxial anisotropy, two permanent magnets were used to supply an external magnetic field of 80 Oe in the film plane during growth. A 5-nm Si_3N_4 protective layer was deposited on the top of the samples by rf sputtering *in situ*. The high-angle x-ray diffraction patterns indicate that NiFe layers exhibit fcc (111) crystalline texture and the SmFe layer is in an amorphous state.

The magnetization hysteresis loops were measured by alternating gradient magnetometer (AGM) in the easy-axis and hard-axis directions. For the samples deposited on the glass substrates, the magnetization hysteresis loops were also measured by the magneto-optical Kerr effect (MOKE). Due to the transparent glass substrates, the $Ni_{80}Fe_{20}/Sm_{40}Fe_{60}$ bilayers can be measured from two sides. Since the penetration depth of light in the metal is about 20 nm and the MOKE signal is mainly from the surface region of a few nanometers, we can almost separately measure the hysteresis loops of NiFe and SmFe layers as long as both layers are not too thin. In this case, MOKE measurements can give additional information about the magnetization reversal. All experiments were conducted at room temperature.

III. MAGNETIZATION-REVERSAL PROCESS NEAR TWO SURFACES AND EXCHANGE BIAS FIELD

Figure 1 shows typical magnetization hysteresis loops measured along the easy and hard axes by MOKE [see Figs. 1(a)–1(d), 1(f), and 1(h)] and AGM [see Figs. 1(e) and 1(g)]. Note that MOKE measurements were carried out from both the NiFe and SmFe sides. For Figs. 1(a) and 1(b), the bilayer thickness is NiFe(6.9 nm)/SmFe(9.7 nm). The easy-axis hysteresis loop and hard-axis loop of the NiFe layer are the same as the corresponding loops for the SmFe layer. This indicates that the magnetic moments in the thin NiFe and SmFe layers always couple together and reverse together. The nearly perfect rectangle of the easy-axis loops and the nearly-hysteresis-free oblique line of the hard-axis loops indicate that a well-defined in-plane uniaxial anisotropy is induced by the external field during film deposition.

For Figs. 1(c) and 1(d), the bilayer thickness is increased to NiFe(17.2 nm)/SmFe(22 nm). The NiFe and SmFe layers have the same easy-axis hysteresis loops, but quite different hard-axis loops. At the maximum of the external field for MOKE measurements (about 1500 Oe), the magnetization of the NiFe soft layer has already approached saturation, but the magnetization of the SmFe hard layer is still far from saturation. This indicates that the magnetic moments in NiFe and SmFe layers can still couple together and reverse together under an external field along the easy axis, whereas an incoherent rotation occurs under an external field along the hard axis.

For Figs. 1(e)–1(h), the bilayer thickness is further increased to NiFe(61.9 nm)/SmFe(87.8 nm). Figures 1(e) and 1(f) are easy-axis loops measured by AGM and MOKE, respectively. Comparing (e) with (f), it is clear that the magnetic moments of the surface of the soft layer first begin to rotate and the soft layer becomes an in-plane domain wall. With increasing reverse field, the domain wall is compressed against the hard/soft interface until the magnetization of the hard layer switches irreversibly. As long as the reverse field is less than the irreversible switching field of the hard layer, the minor loop (a hysteresis loop measured in a small field range after saturation) as shown in Fig. 1(e) is always reversible and shows a bias field from the origin point (0,0) of the main loop.

Figures 1(g) and 1(h) show that the NiFe layer pinned by the interfacial direct exchange coupling is much easier to magnetically saturate than the SmFe layer, and the minor loop is completely reversible and the bias field almost disappears when the external field is along the hard axis. Therefore, the pinned NiFe layer may be used as a nonhysteresis and nearly constant susceptibility material under a small field.

For simplicity, we use the switching field H_{SW} of the minor loop to approximately represent the exchange bias field of the minor loop. Here H_{SW} is defined as the field at which the differential dM/dH has the maximum for the minor loop. Note that the switching field H_{SW} defined as above is different from the nucleation field of the soft layer even for the easy-axis loop. Figure 2 shows the dependence of H_{SW} on the angle between the external field and the easy-axis direction for the NiFe(61.9 nm)/SmFe(87.8 nm) bilayer. For comparison, the coercivity of this bilayer is also shown in Fig. 2. Here H_C is defined as the field at which the magnetization of the main loop is zero. It is clear that the switching field and the coercivity gradually reduce when the angle between the external field and the easy-axis direction increases. A similar angle dependence of the bias field was usually found in ferromagnetic/antiferromagnetic bilayer systems,[12] but here is observed in a soft-ferromagnetic/hard-ferromagnetic bilayer system.

IV. THICKNESS DEPENDENCE OF THE SINGLE-SWITCHING FIELD AND THE NUCLEATION FIELD OF THE SOFT LAYER

Figure 3 shows easy-axis hysteresis loops of the bilayers with various SmFe thicknesses but fixed NiFe thickness. These samples were deposited on glass substrates. For thin SmFe layers, the hysteresis loops only show a single-switching process and the switching field increases when the thickness of the SmFe layer increases, as shown in Figs. 3(a)–3(c). For thick SmFe layers, the exchange spring phe-

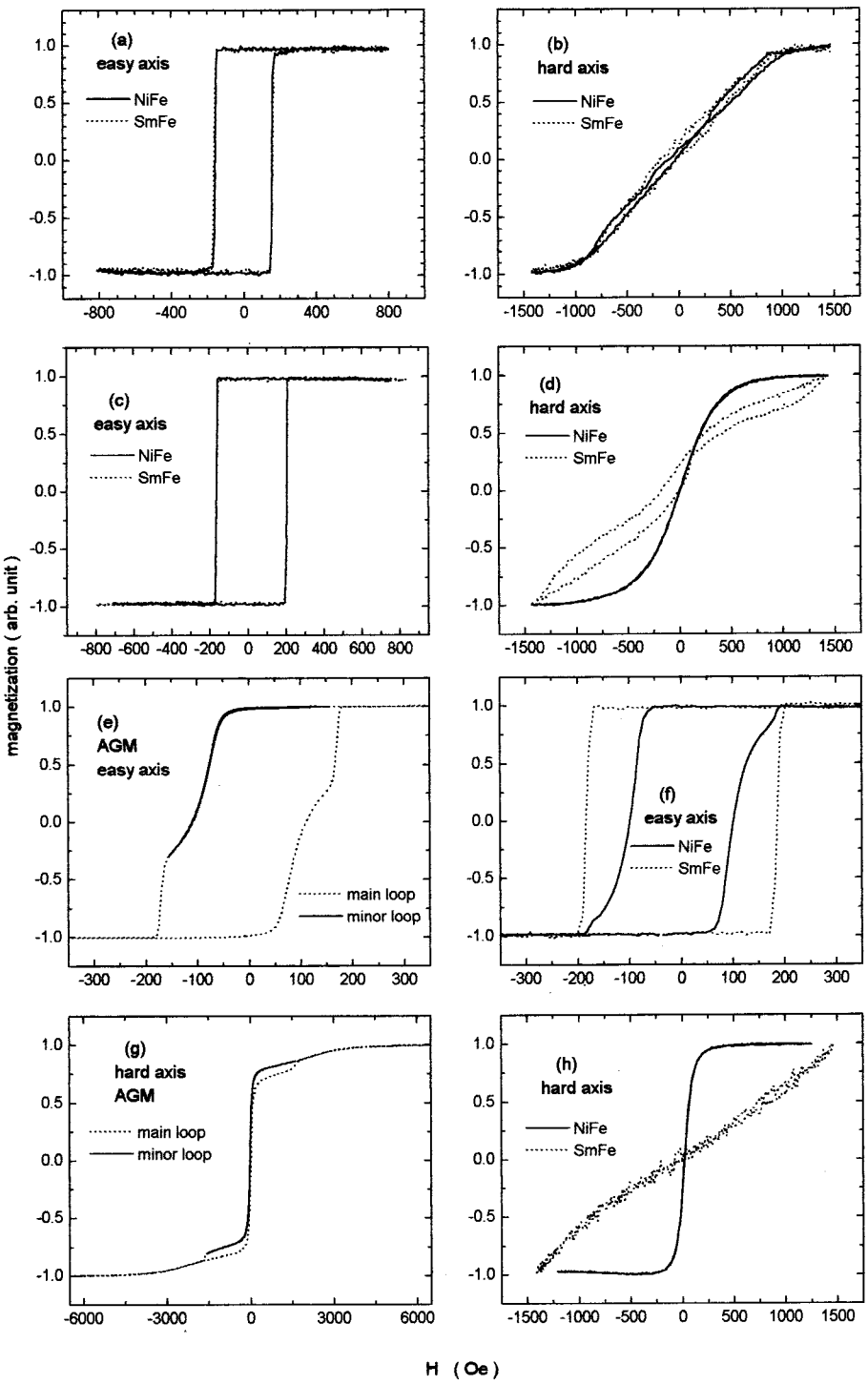

FIG. 1. Typical magnetization hysteresis loops measured along the easy and hard axes by AGM and MOKE. The bilayers were deposited on the glass substrates, and the MOKE measurements are carried out from the NiFe side and SmFe side, respectively. The bilayer thickness is (a) and (b), NiFe(6.9 nm)/SmFe(9.7 nm); (c) and (d), NiFe(17.2 nm)/SmFe(22 nm); (e)–(h), NiFe(61.9 nm)/SmFe(87.7 nm).

nomenon can be found, as shown in Figs. 3(d) and 3(e). In this case the irreversible switching field of the hard SmFe layers increases with increasing SmFe layer thickness. On the other hand, for the fixed NiFe layer thickness, the nucleation field of the soft layer does not change with the hard-layer thickness even if the coercivity and anisotropy of the hard layer changes with its thickness.

Figure 4 shows some typical easy-axis hysteresis loops of the bilayers with various NiFe thicknesses but fixed SmFe thickness. These samples were deposited on (100) Si substrates. For the thin NiFe layers, the hysteresis loops only show a single switching process, and the switching field reduces quickly when the NiFe layer thickness increases, as shown in Figs. 4(a) and 4(b). For thick NiFe layers, the exchange-spring phenomenon can be found, as shown in Figs. 4(c)–4(f). In this case, the nucleation field of the soft NiFe layer quickly reduces when the NiFe layer thickness increases, but the irreversible switching field of the hard SmFe layers remains stable.

The easy-axis coercivity (switching field) of the single-switching process versus the NiFe layer thickness is highlighted in Fig. 5 (partial hysteresis loops have been shown in

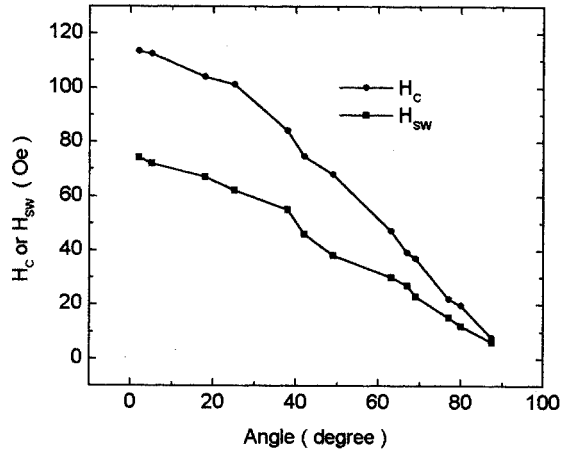

FIG. 2. The dependence of the switching field H_{SW} (approximately representing the exchange bias field) on the angle between the external field and the easy-axis direction for the NiFe(61.9 nm)/SmFe(87.8 nm) bilayer prepared on glass substrate.

Fig. 4). It is clear that the single-switching field monotonously reduces with increasing the NiFe layer thickness up to about 33 nm. According to Ref. 8, Eq. (2) is highly successful in describing the easy-axis coercivity of the single-switching process observed in NiFe/SmFe/NiFe trilayers if both NiFe and SmFe layers are thin. For the present NiFe/SmFe bilayer, a similar formula can be given as follows:

$$H_C = H_0 t_{eh}/(t_{eh} + \alpha t_{es}), \tag{3}$$

where H_0 can be regarded as the coercivity of the single hard layer of the thickness t_h and $\alpha = M_s/M_h$ (M_s is the magnetization of the soft layer and M_h is the magnetization of the hard layer). Note that in Eq. (3) t_{eh} is the effective thickness of the hard layer, and t_{es} is the effective thickness of the soft layer. For the single-switching process described by Eq. (3), t_{es} can always be regarded as the actual physical soft-layer thickness t_s (i.e., $t_{es} = t_s$ for the single-switching process).

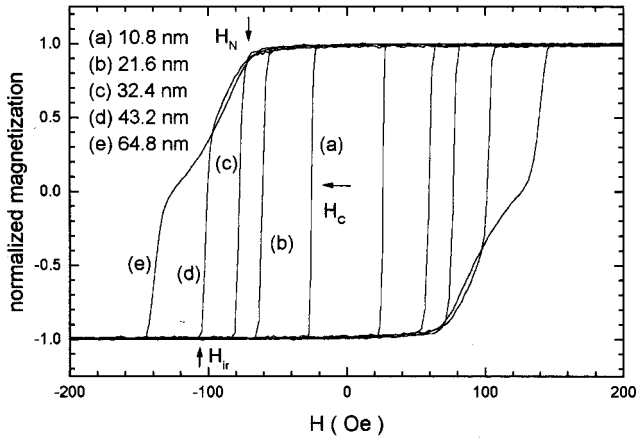

FIG. 3. The easy-axis hysteresis loops of bilayers with various SmFe thicknesses but fixed NiFe thickness (57.6 nm). These samples were deposited on glass substrates. The SmFe layer thickness is (a) 10.8 nm, (b) 21.6 nm, (c) 32.4 nm, (d) 43.2 nm, and (e) 64.8 nm.

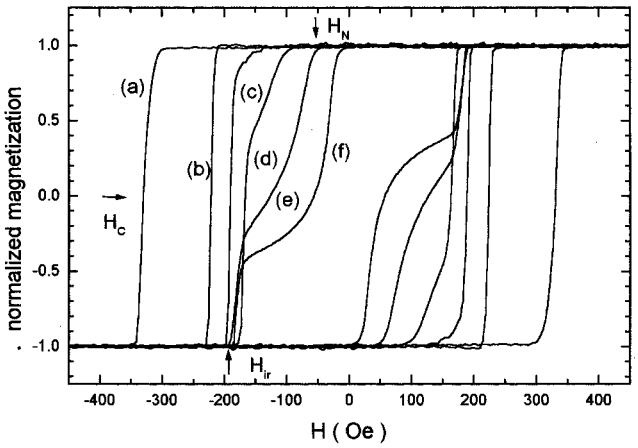

FIG. 4. Some typical easy-axis hysteresis loops of bilayers with various NiFe thicknesses but fixed SmFe thickness (100 nm). These samples were deposited on (100) Si substrates. The NiFe layer thickness is (a) 10.9 nm, (b) 27.2 nm, (c) 34.5 nm, (d) 46.0 nm, (e) 68.9 nm, and (f) 120.6 nm.

There is no doubt that the effective thickness t_{eh} is the actual hard-layer thickness t_h if t_h is thinner than the exchange length l_{exh} of the hard layer (i.e., $t_{eh} = t_h$, if $t_h \leqslant l_{\text{exh}}$). This has been proved in Ref. 8 by the excellent agreement between the experimental easy-axis coercivity and Eq. (2). However, if the actual hard layer is thicker than the exchange length, the effective hard-layer thickness will be limited to this length (i.e., $t_{eh} = l_{\text{exh}}$, if $t_h > l_{\text{exh}}$). Therefore, we fit Eq. (3) to the experimental data of Fig. 5 by a least-square method to obtain H_0 and t_{eh}. It is found that $H_0 = 521$ Oe and $t_{eh} = 55.9$ nm. The agreement between the experimental results (circles) and the fitting (solid line) is very good. The value of $H_0 = 521$ Oe is the same as the easy-axis coercivity of a thick SmFe single film, but $t_{eh} = 55.9$ nm is much less than the actual hard-layer thickness (100 nm). This indicates that once the local NiFe/SmFe bilayer of the exchange length scale begins to unpin, the magnetization of the whole bilayer reverses by domain-wall displacement.

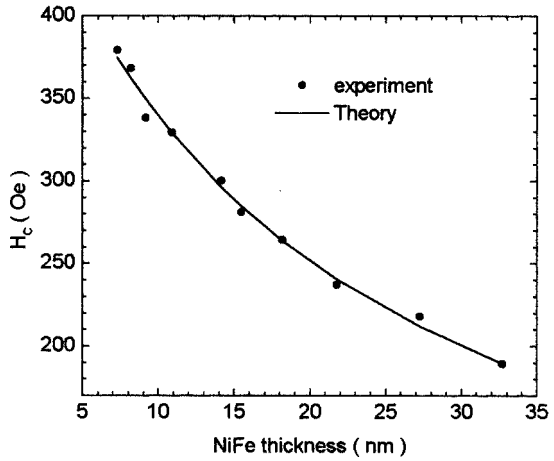

FIG. 5. The easy-axis coercivity (switching field) of the single-switching process versus the NiFe layer thickness. Circles represent the experimental results, and the solid line is the fitting curve using Eq. (3).

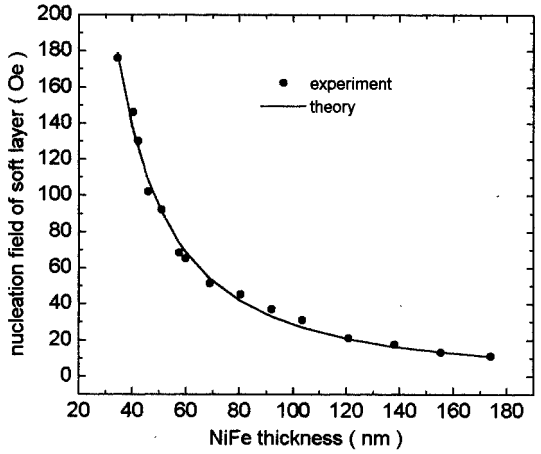

FIG. 6. The nucleation field of the soft layer vs the NiFe layer thickness for the exchange spring process. Circles represent the experimental results, and the solid line is the fitting curve using Eq. (1).

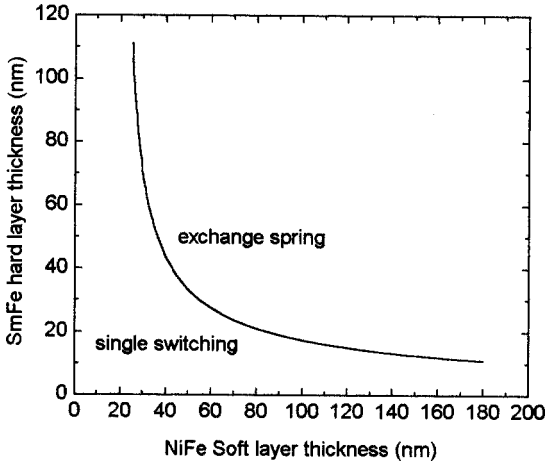

FIG. 7. The critical dimension of the transition from single-switching process to exchange spring process in hard/soft exchange-coupled bilayers. The critical curve is drawn according to Eq. (4), using the values $H_{N0}=8034$ and $H_0=521$ Oe.

The nucleation field of the soft layer versus the NiFe layer thickness is highlighted in Fig. 6 (partial hysteresis loops have been shown in Fig. 4). The nucleation field reduces first quickly and then slowly with increasing NiFe thickness. The experimental data were directly fitted to Eq. (1) by a least-square method. From the fitting, we get the values of $H_{N0}=8034$ (if the unit of thickness is nanometers and the unit of the external field is oersteds) and $n=1.73\pm0.05$. It is clear that the experimental nucleation field is well described by Eq. (1). Moreover, the value of $n=1.73\pm0.05$ is in good agreement with the theoretical value of $n=1.75$.[10]

V. CRITICAL DIMENSION OF THE TRANSITION FROM THE SINGLE-SWITCHING PROCESS TO THE EXCHANGE SPRING

It has been shown in Figs. 3 and 4 that the critical dimension of the transition from the single-switching process to exchange spring depends not only on the soft-layer thickness but also on the hard-layer thickness. For the fixed hard-layer thickness, the single-switching process transfers to the exchange spring process as the soft-layer thickness increases. For the fixed soft-layer thickness, the transition occurs as the hard-layer thickness increases. It has been shown in Fig. 6 that the nucleation field of the soft layer can be well described by Eq. (1). Moreover, Eq. (1) almost does not depend on the hard-layer thickness and its magnetic parameters (such as magnetization, exchange constant, and anisotropy). On the other hand, the single-switching field can be well described by Eq. (3), as shown in Fig. 5. It is clear that Eq. (3) is associated with the structural and magnetic parameters of both hard and soft layers. When the single-switching field determined by Eq. (3) is less than the soft-layer nucleation field determined by Eq. (1), the single-switching field process will occur. When the soft-layer nucleation field determined by Eq. (1) is less than the switching field determined by Eq. (3), the exchange-spring process will occur. At the critical thickness, it is expected that the single-switching field determined by Eq. (3) equals the soft-layer nucleation field determined by Eq. (1). For simplicity, while not losing sight of the essential physics, by neglecting the influence of the exchange length on the effective layer thickness, the effective thicknesses of the layers equal the actual thicknesses in Eq. (3). Combining Eqs. (1) and (3), the critical transition dimensions are obtained as follows:

$$H_N=H_{N0}/(t_s)^n=H_C=H_0t_h/(t_h+\alpha t_s), \tag{4}$$

where H_{N0}, H_0, t_h, t_s, and α are the same as defined before. Equation (4) reveals that any given hard-layer thickness corresponds to a certain critical soft-layer thickness, and vice versa. Assuming H_{N0} and H_0 are two coefficients independent of the thickness of the soft layer and hard layer, the values $H_{N0}=8034$ and $H_0=521$ Oe from the least-square fitting are used in Eq. (4) to construct the phase diagram of magnetization reversal, as shown in Fig. 7. According to Fig. 7, if the hard-layer thickness and the soft-layer thickness are below the critical curve, the magnetization reversal is a single-switching process determined by Eq. (3). If the hard-layer thickness and the soft-layer thickness are above the critical curve, the magnetization reversal is the exchange-spring process and the nucleation field of the soft layer is determined by Eq. (1).

The last problem is how to determine the irreversible switching field of the hard layer. It has been shown in Fig. 4 that the irreversible switching of a given hard layer does not depend on the soft-layer thickness if the soft layer is thicker than a critical thickness. For any given hard-layer thickness, the critical soft-layer thickness can be determined by Eq. (4). Then the irreversible switching field of the hard layer can be determined by this critical soft-layer thickness through Eq. (1) or Eq. (3). This implies that the magnetization-reversal mechanism at the irreversible switching field of the hard layer is the same as that at the single-switching process, i.e., domain-wall unpinning. We think that the compressed domain wall near the interface region unpins locally at the irreversible switching field and quickly sweeps through the

whole sample. However, the details of the domain-wall displacement cannot be determined without domain observation (work in progress). We cannot distinguish whether the locally unpinning domain wall will move only in the film-thickness direction as shown in Fig. 5 of Ref. 6 or if it will move not only in the film thickness direction but also in the film plane as shown in Fig. 3 of Ref. 5.

Summing up the analysis above, for any given hard-layer thickness the critical soft-layer thickness can be determined by Eq. (4). If the actual soft-layer thickness is less than the critical thickness, only the single-switching-field process can be observed and the switching field is determined by Eq. (3). If the actual soft-layer thickness is thicker than the critical thickness, the exchange-spring phenomenon can be observed, the nucleation field of the soft layer is determined by Eq. (1), and the irreversible switching field of the hard layer is determined by the critical thickness through Eq. (1) or Eq. (3). Furthermore, Eq. (1) can be given a more universal explanation: It represents the relationship between the external field and the exchange length (or domain-wall width) of the soft layer under the external field. When the reversed field increases from the nucleation field of the soft layer to the irreversible switching field of the hard layer, the exchange length of the soft layer reduces in terms of Eq. (1). At the nucleation field, the exchange length equals the whole soft layer thickness. At the irreversible switching field, the exchange length is reduced to the critical thickness of the soft layer. In fact, the universal explanation above [or Eq. (1)] resembles the conventional relationship between the external field and the domain-wall width under the field. In particular, in the case of $H_{N0}=\pi^2 A/2M_s$, $n=2$, and $t_s=\pi(A/2M_sH)^{1/2}$, they are identical if the soft layer has no anisotropy.

VI. CONCLUSIONS

The magnetization-reversal process of hard/soft exchange-coupled bilayers is systematically studied by analyzing the magnetic hysteresis loops. In particular, the magnetization-reversal process of the soft layer and hard layer is separately measured by the surface-sensitive MOKE method. The coercivity in the single-switching process and the nucleation field in the exchange spring process are quantitatively described by theoretical models. By doing so, a critical dimension equation describing the transition from a single-switching process to an exchange spring process is achieved. In essence, whether the single-switching process or the exchange spring process will occur is determined by the exchange length (domain-wall width) of the soft layer under a field [Eq. (1)] and the pinning energy exerted on the domain wall of the hard layer [Eq. (3)].

ACKNOWLEDGMENTS

This work was supported by NSF Grant No. DMR-9713497 and DARPA No. DAAD19-01-1-0546. The use of MRSEC shared facilities is also acknowledged (Grant No. DMR-9809423).

*Author to whom correspondence should be addressed. Electronic address: syan@mint.ua.edu

[1] R. Skomski and J. M. D. Coey, Phys. Rev. B **48**, 15 812 (1993).
[2] Eric E. Fullerton, J. S. Jiang, M. Grimsditch, C. H. Sowers, and S. D. Bader, Phys. Rev. B **58**, 12 193 (1998).
[3] A. Ludwig and E. Quandt, J. Appl. Phys. **87**, 4691 (2000).
[4] H. Le Gall, J. Benn Youssef, F. Socha, N. Tiercelin, V. Preobrazhensky, and P. Pernod, J. Appl. Phys. **87**, 5783 (2000).
[5] T. Nagahama, K. Mibu, and T. Shinjo, J. Phys. D **31**, 43 (1998).
[6] S. Mangin, G. Marchal, C. Bellouard, W. Wernsdorfer, and B. Barbara, Phys. Rev. B **58**, 2748 (1998).
[7] S. Wüchner, J. C. Toussaint, and J. Voiron, Phys. Rev. B **55**, 11 576 (1997).
[8] Shi-shen Yan, W. J. Liu, J. L. Weston, G. Zangari, and J. A. Barnard, Phys. Rev. B **63**, 174415 (2001).
[9] E. Goto, N. Hayashi, T. Miyashita, and K. Nakagawa, J. Appl. Phys. **36**, 2951 (1965).
[10] T. Leineweber and H. Kronmüller, J. Magn. Magn. Mater. **176**, 145 (1997).
[11] M. Amato, M. G. Pini, and A. Rettori, Phys. Rev. B **60**, 3414 (1999).
[12] Haiwen Xi, M. H. Kryder, and R. M. White, Appl. Phys. Lett. **74**, 2687 (1999).